

# Bayesian inference of microbiota systems from count metagenomic data

Veronica Vinciotti\*

Department of Mathematics, University of Trento

and

Pariya Behrouzi\*

Department of Mathematics, Wageningen University

and

Reza Mohammadi

Faculty of Economics and Business, University of Amsterdam

## Abstract

Metagenomics combined with high-resolution sequencing have enabled researchers to study the genomes of entire microbial communities. Revealing the underlying interactions between these communities is of vital importance to learn how microbes influence human health. Learning these interactions from microbiome data is challenging, due to the high dimensionality, discreteness, broad dispersion levels, compositionality and excess of zero counts that characterize these data. To tackle these issues, we develop a novel Gaussian copula graphical model with two key elements. Firstly, we model the marginal distributions via discrete Weibull regression, both to account for the typical features of microbiome data and to include the dependency from external covariates, often available in genomic studies but rarely used for network inference. Secondly, we advance a Bayesian structure learning framework, based on a computationally efficient search algorithm that is suited to high dimensionality. The approach returns simultaneous inference of the marginal effects and of the dependency structure, including graph uncertainty estimates. A simulation study and a real data analysis of microbiome data highlight the applicability of the proposed approach at inferring networks from high-dimensional count data in general, and its relevance to microbiota data analyses in particular. The proposed method is implemented in the R package `BDgraph`. Copula graphical models; Discrete Weibull; Link prediction; Microbiome; Structure learning

## 1 Introduction

Interactions between microbes are fundamental in shaping the structure and functioning of the human microbiota, and their malfunctioning has been linked to a number of medical

---

\*These authors contributed equally to this work.

conditions. A lack of understanding of how these interactions shape and evolve makes it difficult to predict their relevance in biomedical fields. For these reasons, microbiota systems have been intensively studied in recent years. Large consortia have developed technologies for the collection of high-throughput data of the microbiome, e.g., the Human Microbiome Project (HMP Consortium, 2012) and the Metagenomics of the Human Intestinal Tract (MetaHIT) project (Qin et al., 2010). These have paved the way for further studies investigating the association of the microbiota functioning with a number of medical conditions, such as obesity (Le Chatelier et al., 2013) and diabetes (Pedersen et al., 2016), as well as with the response to certain treatments, such as immunotherapy (Lee et al., 2022).

Learning these interactions from multivariate data can be achieved via graphical modelling approaches. Among these, Gaussian graphical models are by far the most popular, thanks also to their efficient implementations for high dimensional problems (Friedman et al., 2008; Mohammadi et al., 2021). Microbiome data are however far from Gaussian, with marginal distributions that are in most cases skewed and with a large mass at zero. For this reason, transformations, such as the logarithm or the centered log ratio, are typically applied to the data, followed by Gaussian graphical modelling approaches on the transformed data. This is for example the case of the two most used methods for microbiome data, SparCC (Friedman and Alm, 2012) and SPIEC-EASI (Kurtz et al., 2015), with recent extensions proposing the incorporation of a zero inflated component to the model (Prost et al., 2021).

The transformations above require a pseudo-count adjustment to be able to handle zeros and may also impact the network inference conducted downstream. In the literature, extensions of Gaussian graphical models to non-Gaussian data can take different forms but there is generally little research for the case of unbounded count data, such as the microbiome data. Roy and Dunson (2020) have recently proposed a pairwise Markov random field model with flexible node potentials, while Cougoul et al. (2019) have proposed a Gaussian copula graphical model with zero-inflated negative Binomial marginals, specifically thought for the inference of microbiota systems. Our work is linked to this second paper. On the one hand the use of a Gaussian copula facilitates the integration of novel approaches with existing ones that rely on Gaussianity, without the need for ad-hoc transformations. On the other hand, the use of parametric marginal distributions, rather than the non-parametric empirical distributions as in the popular non-parametric approach (Liu et al., 2009), allows to account for specific features of microbiota data, such as its sparsity and compositional nature, while facilitating the task of incorporating in the model additional covariates, such as the location of the biological sample in the body, which are present in genomic studies but are often ignored due to methodological restrictions.

Copula graphical models describe the joint multivariate distribution of a random vector by coupling the contribution from the marginal distributions with that of the underlying dependency structure. In this paper, we advocate the use of discrete Weibull regression for modelling the marginal distributions and linking these to external covariates (Klakattawi et al., 2018; Haselimashhadi et al., 2018; Peluso et al., 2019). The simplicity of this distribution (a two-parameter distribution), combined with the fact that the two parameters can jointly capture broad levels of dispersion (from under to over), makes it quite an appealing candidate for the high dimensional heterogeneous microbiota data, and in general for multivariate count data with a high number of random variables and/or external covariates. This is because, firstly, for a large number of count variables, one wants to avoid tuning the

type of distribution for each variable, and, secondly, for a large number of external covariates, a global requirement of over dispersion at all levels of the covariates could prove too restrictive. Finally, an important feature of the discrete Weibull distribution in the context of Gaussian copula graphical models, is the fact that it is generated as a discretized form of a continuous Weibull distribution (see Figure 1). This creates a latent non-Gaussian space in the vicinity of the data, with a one-to-one mapping with the latent Gaussian data, where the conditional independence graph resides.

A fundamental problem of copula graphical models for discrete data, bounded or unbounded, is the fact that the marginal distributions are not strictly monotonic. In this setting, while the existence of a copula can still be guaranteed by Sklar’s theorem (Sklar, 1959), its uniqueness can not, leading to potential biases in the inferential procedure. On the one hand, this problem is alleviated by the presence of covariate dependent marginals, particularly when the covariates are continuous and the underlying network does not depend on the covariates (Yang et al., 2020). This can be seen as a second advantage of incorporating covariates in the inferential approaches of microbiota systems, beyond the primary interest of estimating their effect on the microbial abundances, as studied for example in Lee et al. (2020). On the other hand, more advanced inferential procedures are required, that account for the fact that each observed count is associated with an interval in the latent Gaussian space. This relies on the ideas of extended rank likelihood (Hoff, 2007) and has been used also in the context of Gaussian copula graphical models, both in a frequentist setting (Behrouzi and Wit, 2019) and in a Bayesian setting (Dobra et al., 2011; Dobra and Mohammadi, 2018; Mohammadi et al., 2017; Murray et al., 2013).

While extended rank likelihood has been developed for ordinal (bounded) data, in this paper we develop these approaches for Gaussian copula graphical models on unbounded count data with parametric marginals. The use of these approaches avoids the need for ad-hoc data transformation procedures that condense each interval into one point, with choices such as the right-most point of the interval (essentially using the non-paranormal approach of Liu et al. (2009, 2012) on count data) or the point corresponding to the median of the distribution function at the two extremes of the interval (Cougoul et al., 2019). These choices, while efficient, may not work well with skewed distributions, or generally distribution functions that are highly stepwise.

Finally, we conduct inference in a Bayesian framework, leading to a novel Bayesian structure learning procedure in the context of Gaussian copula graphical models with parametric marginals, extending the efficient computational approaches that have been recently proposed for this class of models (Mohammadi and Wit, 2015; Mohammadi et al., 2021). Appropriate choices of a prior distribution on the graphs can be made to encourage sparsity. Importantly, uncertainty on the graph learning is fully quantified by the procedure and can be summarized in various ways, such as by calculating posterior probabilities for each edge via Bayesian averaging. This has not been done before in the analysis of microbiota systems, and plays a crucial role, particularly in high dimensional settings.

In conclusion, this paper presents a novel methodology for the inference of microbiota systems from high dimensional metagenomic count data, characterized by broad dispersion levels, compositionality and excess of zero counts. Section 2 will describe the details of the methodology proposed, whose implementation has been included in the R package `BDgraph` (Mohammadi and Wit, 2019). A simulation study in Section 3 and a real data analysis of microbiome data from the HMP in Section 4 will show the usefulness of the

proposed approach at inferring networks from high-dimensional count data in general, and in the context of microbiota data analyses in particular. Finally, Section 5 will draw some conclusions and point to future research directions.

## 2 Methods

In this section, we present the technical details of the proposed method, starting with the definition of a Gaussian copula graphical model and of the discrete Weibull (DW) regression used for the marginal components, followed by the Bayesian inferential procedure.

### 2.1 Gaussian copula graphical model with DW marginals

Let  $\mathbf{Y} = (Y_1, \dots, Y_p)$  be a vector of count variables. In the case of microbiota systems, these are abundances of the individual microbes or, more commonly, of the Operating Taxonomic Units (OTUs) into which they are clustered, e.g., bacterial species. Let  $F_j(\cdot)$ ,  $j = 1, \dots, p$ , be the distribution functions associated to the  $p$  variables, respectively. In a copula graphical model, the joint distribution of the variables is described via a copula function  $C(\cdot)$  that couples the marginal distributions  $F_j(\cdot)$  into their joint dependency. Formally,

$$P(Y_1 \leq y_1, \dots, Y_p \leq y_p) = C(F_1(y_1), \dots, F_p(y_p) | \Theta),$$

where  $\Theta$  are the parameters describing the copula function  $C(\cdot)$ . In the case of a Gaussian copula (Hoff, 2007; Mohammadi et al., 2017)

$$P(Y_1 \leq y_1, \dots, Y_p \leq y_p) = \Phi_p(\Phi^{-1}(F_1(y_1)), \dots, \Phi^{-1}(F_p(y_p)) | \mathbf{R}),$$

where  $\Phi_p(\cdot)$  is the cumulative distribution function of a  $p$ -dimensional multivariate normal with a zero mean vector and correlation matrix  $\mathbf{R}$ , while  $\Phi(\cdot)$  is the standard univariate normal distribution function. The dependency structure is captured by the inverse of the correlation matrix  $\mathbf{K} = \mathbf{R}^{-1}$ , typically called the precision or concentration matrix. In particular, the zero patterns in this matrix define the conditional independence graph in the latent Gaussian space, following from the theory of Gaussian graphical models (Lauritzen, 1996).

In the context of copula graphical models, the marginal distributions  $F_j(\cdot)$  are typically considered as nuisance parameters and estimated by their empirical counterpart. However, in real-world applications, such as in genomic studies, external covariates are often available and there is an interest in estimating their effect on the outcome while accounting for the multivariate nature of the data. Moreover, the inclusion of covariates in the marginal components of a copula graphical model on discrete data facilitates the recovery of the underlying conditional dependency structure.

In this paper, we propose to model the marginal components, and their link with covariates, via a discrete Weibull regression (Peluso et al., 2019). Formally, let  $\mathbf{X} = (1, X_1, \dots, X_d)$  be a vector of covariates. Then, the conditional distribution of  $Y_j$  given  $\mathbf{X}$  is modelled by:

$$F_j(y_j | \mathbf{X} = \mathbf{x}) = 1 - q_j(\mathbf{x})^{(y_j+1)^{\beta_j(\mathbf{x})}}, \quad y_j = 0, 1, \dots, \quad (1)$$

where the function  $q_j(\cdot)$ , corresponding to the parameter  $q$  of the distribution, takes values between 0 and 1, while  $\beta_j(\cdot)$  is associated to the parameter  $\beta$  and takes values in the positive real line. We link the parameters to the external covariates using the logit and the log links, respectively, that is

$$\log\left(\frac{q_j(\mathbf{x})}{1 - q_j(\mathbf{x})}\right) = \mathbf{x}^t \boldsymbol{\theta}_j, \quad \log(\beta_j(\mathbf{x})) = \mathbf{x}^t \boldsymbol{\gamma}_j, \quad (2)$$

with  $\boldsymbol{\theta}_j$  and  $\boldsymbol{\gamma}_j$  denoting the regression coefficients associated to the  $Y_j$  marginal component of the model. For other choices of link functions, see Haselimashhadi et al. (2018). The simplest case of only the intercept in each model corresponds to the case of no external covariates, i.e., simply discrete Weibull marginal distributions. In the real data analysis, we also consider a model with an additional zero inflation parameter  $\pi_j$ , as in Burger et al. (2020). This is common in the microbiome literature due to the sparsity of the data (Cougoul et al., 2019), although we find that this zero-inflated model is rarely selected against the simpler model.

A few properties of a discrete Weibull distribution make it an ideal candidate for modelling high dimensional count data. In particular:

1.  $F_j(0|\mathbf{X} = \mathbf{x}) = P(Y_j = 0|\mathbf{X} = \mathbf{x}) = 1 - q_j(\mathbf{x})$ , thus the parameter  $q$  models directly the proportion of zeros in the data and the effect of covariates on this.
2. The two parameters of the distribution are sufficient to capture both under and over dispersion levels, while still being a parsimonious choice (e.g., same number of parameters as the commonly used negative Binomial distribution). This has been shown to be useful on real data analyses of count data, particularly in the case of under dispersion (Peluso et al., 2019). Although microbiome data are typically highly over dispersed, the presence of a large number of external covariates could make a global requirement of over dispersion at all levels of the covariates  $\mathbf{x}$  too restrictive. Moreover, capturing both over and under dispersion is appealing when modelling any generic high dimensional multivariate count data, as it avoids the fine tuning of the most appropriate marginal distribution for each variable.
3. The quantiles of the distribution have a closed-form expression, with the  $\tau$  quantile, for  $\tau \geq 1 - q$ , given by (Peluso et al., 2019),

$$\mu_{(\tau)} = \left\lceil \left( \frac{\log(1 - \tau)}{\log(q)} \right)^{1/\beta} - 1 \right\rceil,$$

where  $\lceil \cdot \rceil$  denotes the ceiling function. This means that a re-parametrization based on the median is also possible, e.g., when quantification of the covariate effects is of primary interest (Burger et al., 2020).

4. The distribution is developed as a discretized form of the continuous Weibull distribution (Chakraborty, 2015). Namely, by defining the cumulative distribution function (cdf) of a continuous Weibull distribution by

$$F_{CW}(y; q, \beta) = 1 - \exp \left[ - \left( \frac{y}{(-\log q)^{-\frac{1}{\beta}}} \right)^\beta \right], \quad y \geq 0,$$

one can easily show that the probability mass function of the discrete Weibull distribution, associated to the cdf in Equation 1, is given by

$$f(y; q, \beta) = q^{y^\beta} - q^{(y+1)^\beta} = F_{CW}(y+1) - F_{CW}(y) = \int_y^{y+1} f_{CW}(t) dt \quad y = 0, 1, 2, \dots$$

This creates a one-to-one connection between the latent continuous Weibull space, with the same parameters as the discrete Weibull distribution, and the Gaussian space, as depicted schematically in Figure 1.

As it is clear also from the figure, each discrete observation is linked to an interval in the continuous space. This is the case for copula models on discrete data in general and will require special attention when it comes to inference, as we will discuss more in details in the next section.

## 2.2 Bayesian inference for a DW graphical model

Inference for copula graphical models involves estimation of the marginals and of the network component. A copula formulation enables us to learn the marginals separately from the dependence structure of the  $p$ -variate random variables.

We first concentrate on the marginal components, that is the estimation of the regression coefficients  $\boldsymbol{\theta}_j$  and  $\boldsymbol{\gamma}_j$ ,  $j = 1, \dots, p$ . Given  $n$  observations on component  $Y_j$ , denoted with the vector  $\mathbf{y}_j$ , and on the  $d$ -dimensional vector of covariates, stored in the  $n \times d$  matrix  $\mathbf{x}$  with  $\mathbf{x}_i$  the vector corresponding to the  $i^{th}$  row, the likelihood for component  $j$  is given by

$$L_j(\mathbf{y}_j, \mathbf{x} \mid \boldsymbol{\theta}_j, \boldsymbol{\gamma}_j) = \prod_{i=1}^n \left[ \left( \frac{e^{\mathbf{x}_i^t \boldsymbol{\theta}_j}}{1 + e^{\mathbf{x}_i^t \boldsymbol{\theta}_j}} \right)^{y_{ij}^{(e^{\mathbf{x}_i^t \boldsymbol{\gamma}_j})}} - \left( \frac{e^{\mathbf{x}_i^t \boldsymbol{\theta}_j}}{1 + e^{\mathbf{x}_i^t \boldsymbol{\theta}_j}} \right)^{(y_{ij}+1)^{(e^{\mathbf{x}_i^t \boldsymbol{\gamma}_j})}} \right],$$

where we consider the logit and log links on the  $q$  and  $\beta$  parameters, respectively. Based on this likelihood, we perform inference on the marginal components using an adaptive Metropolis-Hastings scheme, as in Haselimashhadi et al. (2018). For the simulations and real data analysis in this paper, we set standard Gaussian priors on the regression coefficients  $\boldsymbol{\theta}_j$  and  $\boldsymbol{\gamma}_j$ .

Once the marginals are estimated, inference of the network component requires an inverse mapping from the observed to the latent Gaussian space. As depicted visually in Figure 1, each observed discrete value corresponds to an interval in the latent Gaussian space with the same associated probability. Formally, given the  $n \times p$  observed data  $\mathbf{y}$  and the fitted marginals, the Gaussian latent variables  $\mathbf{z}$  are constrained in the intervals

$$\mathcal{D}_F(\mathbf{y}) = \{ \mathbf{z} \in R^{n \times p} : \Phi^{-1}(F_{ij}(y_{ij} - 1)) < z_{ij} \leq \Phi^{-1}(F_{ij}(y_{ij})) \},$$

where we indicate with  $F_{ij}$  the cdf of  $Y_j$  when  $\mathbf{X} = \mathbf{x}_i$ . Rather than condensing these intervals into a single point, as in Cougoul et al. (2019), we retain this information within the MCMC sampling scheme, similar to the approach of Dobra et al. (2011) and Mohammadi et al. (2017) for ordinal data.

In particular, the extended rank likelihood function for a given graph  $G$  and associated precision matrix  $\mathbf{K} = \mathbf{R}^{-1}$  is defined as

$$L_E(\mathbf{z} \in \mathcal{D}_F(\mathbf{y}); \mathbf{K}, G) = \int_{\mathcal{D}_F(\mathbf{y})} P(\mathbf{z} | \mathbf{K}, G) d\mathbf{z}$$

where  $P(\mathbf{z} | \mathbf{K}, G)$  is the profile likelihood in the Gaussian latent space:

$$P(\mathbf{z} | \mathbf{K}, G) \propto |\mathbf{K}|^{n/2} \exp\left\{-\frac{1}{2}\text{Tr}(\mathbf{K}\mathbf{U})\right\}$$

with  $\mathbf{U} = \mathbf{z}^t \mathbf{z}$  the sample moment. The likelihood is combined to priors to lead to the posterior

$$P(\mathbf{K}, G | \mathbf{z} \in \mathcal{D}_F(\mathbf{y})) \propto L_E(\mathbf{z} \in \mathcal{D}_F(\mathbf{y}); \mathbf{K}, G) P(\mathbf{K} | G) P(G) \quad (3)$$

where  $P(\mathbf{K} | G)$  denotes the prior distribution on the precision matrix  $\mathbf{K}$  for a given graph structure  $G$  and  $P(G)$  denotes a prior distribution for the graph  $G$ .

As regards to the prior specification on the graph  $G$ , we consider an Erdős-Rényi random graph with a prior probability of a link  $\pi \in (0, 1)$  (which we set to 0.5, representing the case of a noninformative prior, unless stated otherwise). For other options, see Dobra et al. (2011) and Mohammadi and Wit (2015). As for the precision matrix  $\mathbf{K}$ , conditional on a given graph  $G$ , we consider a G-Wishart distribution, defined by

$$P(\mathbf{K} | G) = \frac{1}{I_G(b, \mathbf{D})} |\mathbf{K}|^{(b-2)/2} \exp\left\{-\frac{1}{2}\text{tr}(\mathbf{D}\mathbf{K})\right\},$$

where  $b > 2$  is the degree of freedom,  $\mathbf{D}$  is a symmetric positive definite matrix, and  $I_G(b, \mathbf{D})$  is a normalizing constant (Roverato, 2002). For the simulations and real data analysis in this paper, we set a  $W_G(3, \mathbb{I}_p)$  prior distribution, following Mohammadi et al. (2021).

As the space of possible graphs is very large, computationally efficient search algorithms are needed to sample from the posterior distribution (3). To efficiently explore the graph space, Mohammadi and Wit (2015) developed a birth-death Markov chain Monte Carlo (BDMCMC) search algorithm, in which the algorithm explores the graph space by either adding (birth) or deleting (death) an edge to a graph  $G = (V, E)$ , independently of the rest and via a Poisson process with birth/death rates given by

$$R_e(G, \mathbf{K}) = \min\left\{\frac{P(G^*, \mathbf{K}^* | \mathbf{z})}{P(G, \mathbf{K} | \mathbf{z})}, 1\right\}, \text{ for each } e \in \{E \cup \bar{E}\}, \quad (4)$$

where  $G^* = (V, E \cup \{e\})$  for the birth of an edge  $e \in \bar{E}$ , while  $G^* = (V, E \setminus \{e\})$  for the death of an edge  $e \in E$ , and  $\mathbf{K}^*$  is the corresponding precision matrix. Since the birth/death events are independent Poisson processes, the time between two successive events has a mean waiting time given by

$$W(G, \mathbf{K}) = \frac{1}{\sum_{e \in \{E \cup \bar{E}\}} R_e(G, \mathbf{K})}. \quad (5)$$

Based on the above birth/death rates and waiting times, the birth and death probabilities that govern the move to a new graph are given by

$$P(\text{birth/death of edge } e \in \{E \cup \bar{E}\}) = R_e(G, \mathbf{K}) \times W(G, \mathbf{K}). \quad (6)$$

The pseudo-code for the BDMCMC search algorithm for sampling from the target posterior distribution (3) is reported in Algorithm 1. The first step of Algorithm 1 is to

---

**Algorithm 1:** BDMCMC search algorithm for GCGM with DW marginals

---

**Input:** A graph  $G = (V, E)$  with a precision matrix  $\mathbf{K}$  and data  $\mathbf{y}$  and  $\mathbf{x}$ .

**for**  $N$  iteration **do**

**Step 1:** Sample the latent data for each marginal  $j$ , updating the latent  $n$  values  $\mathbf{z}_j$  from their full conditional distribution:

$$Z_j | \mathbf{K}, \mathbf{Z}_{V \setminus \{j\}} = \mathbf{z} \sim N\left(-\sum_k \frac{K_{jk} z_k}{K_{jj}}, \frac{1}{K_{jj}}\right),$$

each truncated on its corresponding interval  $\mathcal{D}_{F_j}(\mathbf{y}_j)$  with  $F_j(\cdot)$  fitted via a discrete Weibull regression model linking  $\mathbf{y}_j$  to  $\mathbf{x}$ ;

**Step 2: for all the possible jumps in parallel do**

    | Compute the birth and death rates by Equation 4;

    Compute the waiting time by Equation 5;

    Sample the graph based on the birth/death probabilities in Equation 6;

**Step 3:** Sample the precision matrix, according to the updated graph;

**Output:** Samples from the target posterior distribution (3).

---

update the latent variables given the observed data. Then, in step 2, on the basis of the sampled latent data, the algorithm computes the birth/death rates. This is done in parallel since the rates associated to each edge can be calculated independently of each other; for details on how to calculate the birth/death rates see (Mohammadi et al., 2021, Section 2), while Figure 2 provides a visualization of the algorithm. Finally, step 3 of the algorithm can be done by exact sampling from a G-Wishart distribution, as in Lenkoski (2013).

Following from the Bayesian inference of the Gaussian copula graphical model with discrete Weibull marginals, one can extract any information of interest for the analysis. In particular, from the marginal components, one obtains the posterior distribution of the regression coefficients and can investigate any effect of interest, while from the graph posterior, one can calculate the posterior edge inclusion probabilities:

$$P(\text{edge } e \in E \mid \text{data}) = \frac{\sum_{t=1}^N 1(e \in G^{(t)}) W(G^{(t)}, \mathbf{K}^{(t)})}{\sum_{t=1}^N W(G^{(t)}, \mathbf{K}^{(t)})}, \quad (7)$$

where  $N$  denotes the MCMC iterations (after burn-in) and  $1(e \in G^{(t)}) = 1$  if  $e \in G^{(t)}$  and zero otherwise. These probabilities capture the full uncertainty on the graph learning, which is particularly useful in high dimensional settings such as the microbiome data.



### 3 Simulation study

The main objective of the proposed method is that of learning the underlying structure of dependency from complex and heterogeneous count data, which are routinely generated in genomic studies. We therefore conduct a simulation study to measure the performance of the method in terms of graph recovery and to test its robustness to marginal distributions different from discrete Weibull.

For the simulations, we consider networks with  $p = 100$  nodes and a random graph structure with a 20% sparsity. Given a graph  $G$  and marginals  $F_j(\cdot)$ ,  $j = 1, \dots, p$ , we use the following procedure to simulate count data. We first generate a precision matrix from a G-Wishart distribution, namely  $\mathbf{K} \sim W_G(3, \mathbb{I}_p)$ , and standardize it to the inverse of a correlation matrix. We then draw  $n = 100$  multivariate normal samples from  $N_p(\mathbf{0}, \mathbf{K}^{-1})$ . This generates a matrix  $\mathbf{Z}$  of dimension  $n \times p$ . Finally, we obtain the discrete data using  $y_{ij} = F_j^{-1}(\Phi(z_{ij}))$ , for  $i = 1, \dots, n$  and  $j = 1, \dots, p$ , with  $\Phi(\cdot)$  the standard normal distribution and  $F_j(\cdot)$  a distribution function of a specified shape as explained below.

Given a binary external covariate  $X$  drawn from a Bernoulli(0.5), e.g., observations split into two groups as in the real data analysis (two environments: stool and saliva), we simulate marginals in the following three settings:

1. DW under-dispersed with  $\log(\beta(x)) = \gamma_0 = \log(2.5)$  (not dependent on  $X$ ) and  $\log(q(x)/(1 - q(x))) = \theta_0 + \theta_1 x$ , with  $\theta_0 = \log(0.85/(1 - 0.85)) = 1.734$  and three cases for  $\theta_1$  capturing increasing levels of dependency on  $X$ , namely  $\theta_1 \in \{0, 1, 2\}$ ;
2. DW over-dispersed with  $\log(\beta(x)) = \gamma_0 = \log(0.7)$  (not dependent on  $X$ ) and  $\log(q(x)/(1 - q(x))) = \theta_0 + \theta_1 x$ , with  $\theta_0 = \log(0.5/(1 - 0.5)) = 0$  and  $\theta_1 \in \{0, 1, 2\}$ ;
3. NB with similar mean and variance levels to the previous case across the three settings. This was obtained by setting the dispersion parameter  $\phi = 0.5$  and  $\log(\mu) = \theta_0 + \theta_1 x$ , with  $\theta_0 = \log(2) = 0.693$  and  $\theta_1 \in \{0, 1.2, 2.5\}$ .

We compare the following three approaches. Firstly, we consider our own method, a Gaussian copula graphical model with discrete Weibull marginals, defined by Equation (2) and that we abbreviate to DWGM. We run the Bayesian inferential procedures for 10k iterations for each marginal and 500k iterations for the structure learning (Algorithm 1), and set the priors as specified in the description of the method. Secondly, we consider the Bayesian Gaussian copula graphical model (GCGM) for ordinal data of Mohammadi et al. (2017), implemented in the R package `BDgraph`. We use 500k iterations also in this case and the same prior specifications. In the absence of covariates, the GCGM method is similar to our approach, the only difference being the (non-parametric) empirical marginal distributions used in GCGM versus the parametric distributions with an unbounded support for the marginals in DWGM. Clearly, being non-parametric, GCGM does not allow the explicit inclusion of covariates in the marginals. Thirdly, we consider the parametric approach of Cougoul et al. (2019), implemented in the R package `rMAGMA`, which uses zero-inflated negative Binomial distributions for the marginals, with a constant dispersion parameter for each marginal and a mean dependent on the covariates. As well as using a different distribution for the marginals, inference in `rMAGMA` is conducted using a frequentist paradigm and, in addition, it does not make use of the extended rank likelihood approach. Indeed, the fitted marginals are used to transform the data into the latent variables by taking the mean of

the interval, i.e.,  $z_{ij} = \Phi^{-1}\left(\frac{F_j(y_{ij} - 1) + F_j(y_{ij})}{2}\right)$ , and then graphical lasso is used on the transformed data.

We evaluate the performance of the methods in terms of the area under the associated Receiver Operating Characteristic (ROC) curve. For **DWGM** and **GCGM**, this is obtained by setting cutoffs on the posterior edge inclusion probabilities in Equation 7. For **rMAGMA**, which is based on penalised inference, the ROC curve is constructed across the path of solutions generated by the tuning penalty parameter.

Figure 3 shows the AUC values for the three settings, across 50 simulated datasets for each setting. For the parametric models, we consider both a model that includes covariates in the marginals and a model without covariates, i.e., a model with DW marginals in the case of **DWGM** and NB marginals in the case of **rMAGMA**. The results show, firstly, how **DWGM** and **GCGM** are overall superior to **rMAGMA**, even in the case of negative Binomial marginals, when **rMAGMA** is correctly specified. Since **rMAGMA** is the only frequentist approach of the three, we speculate that the posterior edge probabilities lead to a better separation between the presence/absence of links than the edge weights calculated across the penalised path of **rMAGMA**. Secondly, the non-parametric **GCGM** approach performs well in the absence of covariates ( $\theta_1 = 0$ ), even when compared with the correct parametric models. Thirdly, parametric models that include covariates perform similarly or better than the corresponding methods that do not account for covariates, with an out-performance that increases the more pronounced the covariate effect is, i.e., as  $\theta_1$  increases. Indeed, not correcting for the covariates at the marginal level may result in the detection of spurious interactions between the variables (Vinciotti et al., 2016), and thus lead to a poorer graph recovery. The setting with the largest  $\theta_1$  shows a clear out-performance of **DWGM** compared to all the other methods.

## 4 Inferring the network of the microbiota

In this section, we use Gaussian copula graphical models with discrete Weibull marginals to recover the network of interactions between microbial species. As in Cougoul et al. (2019), we retrieve the 16S variable region V3-5 data from the Human Microbiome Project (HMP Consortium, 2012) and perform the analysis at the level of Operating Taxonomic Units (OTUs). After filtering samples with less than 500 reads, we consider microbiomes from 663 healthy individuals, with microbial concentration measured from either stool or saliva. We then restrict our attention to the 155 OTUs which are present in at least 25% of the samples and with more than two distinct observed values in both the saliva and stool samples. These are the nodes of the network.

The microbial communities in the mouth and colon are connected anatomically via the saliva. However, the extent to which oral microbes reach and colonize the gut is yet under debate (Rashidi et al., 2021). To resolve this long-standing controversy, many studies have been devoted to study jointly the human stool and saliva microbiome profiles. To this end, we apply our methodology to recover a network of interactions between microbes across the different environments. Crucially, the method takes into account both the fact that the OTU abundances may differ marginally between the body sites (stool and saliva) and that the data may be affected by potential experimental effects. Indeed, in the case of microbiome data, it is well known how sequencing depths change significantly between

samples. To this end, we estimate the library size of each sample by the geometric mean of pairwise ratios of OTU abundances of that sample with all other samples (Cougoul et al., 2019).

## 4.1 Accounting for covariates via DW regression marginals

We use the estimated library size as one covariate in the marginal regression models, together with the body site covariate, indicating whether a sample is from stool or saliva. We fit discrete Weibull marginal models, linking both parameters  $q$  and  $\beta$  to the covariates as described previously, i.e., 6 parameters per marginal component. We use 300k MCMC iterations, retaining the last 25% as samples from the posterior distribution. As the data are sparse (with a percentage of zeros per OTU ranging from 40.7% to 75%), we fit also a zero-inflated discrete Weibull distribution, with a constant zero inflation parameter  $\pi_j$  for component  $j$ , on which we place a Beta(1,1) prior distribution. Comparing the zero-inflated versus the standard DW regression model using the Bayesian Information Criterion (BIC), we found that 33 out of the 155 OTUs necessitated the zero-inflated component of the model. As a matter of comparison, we also fitted negative Binomial, using its most common formulation with a mean dependent on the covariates and a constant dispersion parameter, as in Cougoul et al. (2019). Here we found that 11 out of the 155 OTUs were better fitted with a zero-inflated NB model. These results show how using a zero-inflated model upfront because the data are very sparse, as done in most of the literature on microbiome analyses, may not necessarily be the best option.

Figure 4 shows how a discrete Weibull regression model has, for most OTUs, a lower BIC than a negative Binomial regression model (where we consider in each case the BIC of the best model between the zero-inflated and the non-zero inflated version), with various cases showing a significantly better fit for DW. In the right plot, we calculate the dispersion ratio (i.e., the variance divided by the mean) from the fitted DW marginals for each observation and each OTU. The plot shows how the data are highly over-dispersed in both conditions, a setting where NB is typically the default choice. Finally, the bottom plots show the OTU with the largest BIC difference, i.e., the OTU best fitted by DW when compared to NB. Here, we plot the cumulative distribution functions of DW and NB associated to the two body sites, while taking an average of the parameters across the normalizing factor. Superimposing these on the empirical cumulative distribution functions associated to the two groups, we see how discrete Weibull shows a better fit overall.

Including covariates in the inference of microbiota systems has the advantage that analyses that are typically conducted on a microbe by microbe basis are now naturally embedded in the overall joint model. Indeed, one can inspect the estimation and inference of any marginal effect of interest. In this particular analysis, there is interest in detecting the OTUs that are differentially expressed between the two different body sites. Figure 5 shows how all 155 OTUs differ significantly between the two body sites. Furthermore, the plots show how the regression coefficient of the  $q$  parameter is highly significant, suggesting large differences between the proportion of zeros in the two environments for most OTUs. In contrast to this, the regression coefficient of the  $\beta$  parameter is less significant. This may in fact indicate that a simpler DW regression model, with a constant  $\beta$  parameter, may be sufficient for some of the OTUs.

## 4.2 Bayesian structure learning of the microbiota system

We now turn to the task of recovering the underlying network of dependencies between the OTUs. The space of possible graphs among 155 nodes is huge, creating a statistical and computational challenge at a level that has not been considered before in the context of Bayesian structure learning. Thus a few checks and considerations were made. Firstly, we start the MCMC chain by setting the initial graph to the graph detected by **rMAGMA** using zero-inflated negative Binomial as marginals and the stability selection criterion **stars** for model selection (Liu et al., 2010). Secondly, we perform the structure learning for a long number of iterations, namely 10 million MCMC iterations, making use of a high performance computing cluster. Thirdly, we run five parallel chains, in order to check if there is convergence to similar graphs. We also check the sensitivity to the graph prior, by setting the edge probability  $\pi$  to 0.04 (i.e., a high sparsity, at the level of the initial graph detected by **rMAGMA**) for two of the chains and the default value of 0.5 for the other three. Overall, we observe a very high correlation among the edge posterior probabilities from the two chains with  $\pi = 0.04$  (0.96) and from the three chains with  $\pi = 0.5$  (ranging from 0.85 to 0.88), and lower but still high correlations between the two groups of simulations (ranging from 0.63 to 0.64). For the rest of the analysis, we consider the chain that resulted in the highest log-likelihood when evaluated at the posterior estimates of the marginal distributions and precision matrix.

We firstly investigate the impact that the inclusion of covariates has on the inference of the underlying graph. The expectation is that unaccounting for potential differences between the two environmental sites will lead to the detection of spurious interactions. To this end, we compare our proposed approach with a Gaussian copula graphical model that uses the empirical distribution for the marginals (**GCGM**), i.e., a model that does not make use of covariate information. We run also **GCGM** using 10 million iterations for the structure learning part and using the same prior on the graph ( $\pi = 0.04$ ). Figure 6 shows how the posterior distribution on graph sizes from the **DWGM** model (left) is concentrated on a sparser graph compared with the posterior distribution from the **GCGM** model, suggesting spurious links being detected by this second analysis where covariates have been omitted. As a side effect, **GCGM** has also a much higher computational time (224 hours versus 124 hours for **DWGM** on the same cluster), since the computational time of these structure learning methods is correlated with the sparsity level of the graphs that are sampled.

Setting a cutoff of 0.5 on the edge posterior probabilities, the network contains 355 edges. Figure 7 shows the overlap between these edges and the optimal graph detected by **rMAGMA** (Cougoul et al., 2019). There is a moderate (185 edges) overlap with the total of 414 edges detected by **rMAGMA**. One of the major advantages of **DWGM**, which has not been considered before in the context of microbiome analyses, is that the uncertainty around the optimal graph is also measured. This is particularly important for structure learning in high dimensions. Indeed, the right plot of Figure 7 shows how many of the edges detected by **rMAGMA** have a low posterior edge probability calculated by **DWGM**.

Finally, Figure 8 plots the network inferred by **DWGM**, with nodes coloured according to their phyla association (firmicutes, proteobacteria, bacteroidetes, actinobacteria, fusobacteria) and edges coloured according to their partial correlations, computed from the Bayesian averaging estimate of the precision matrix. The information on phyla association is useful in distinguishing between the stool and saliva microbiota. Indeed, firmicutes and

bacteroidetes represent more than 90% of the total human gut microbiota (Qin et al., 2010) and have been found associated with several pathological conditions affecting the gastrointestinal tract, obesity and type 2 diabetes (Magne et al., 2020; Indiani et al., 2018). So we take this group of OTUs as representative of the gut microbiota. The remaining OTUs, with a mix of phylum levels, are instead associated to the saliva microbiota (Choi et al., 2020). In the optimal network (Figure 8), more connections are found within each group (average posterior edge probability equal to 4.8% in gut and 10% in saliva) than between the two groups (average posterior edge probability equal to 1.7% between gut and saliva). While the connections are particularly strong within each group (average of posterior edge probabilities larger than 0.5 equal to 88% in gut and 90% in saliva, with associated average absolute partial correlation equal to 0.23 and 0.22, respectively), strong connections are detected also between the two groups (average of posterior edge probabilities larger than 0.5 between gut and saliva equal to 80%, with associated average absolute partial correlations equal to 0.17), suggesting the presence of interactions between the two systems and supporting existing knowledge that oral microbes have the capacity to spread throughout the gastrointestinal system.

## 5 Conclusion

In this paper, we have presented a copula graphical modelling approach that is able to recover the network of interactions between microbes from count data provided by the latest microbiome experiments and featuring high dimensionality, sparsity, heterogeneity and compositionality. The approach has three key features.

Firstly, it allows to adjust for the effect of covariates in the marginal components of the model. This is useful, both in quantifying the effect of covariates of interest on microbial abundances and in aiding network recovery. The latter is down to two reasons: on one hand, the inclusion of covariates removes spurious dependencies that may be induced by the effect of the covariates on the microbial abundances; on the other hand, the inclusion of (particularly continuous) covariates at the marginal level expands the region of support for consistent estimation of the copula in the case of discrete variables.

Secondly, discrete Weibull regression is used for modelling the marginal distributions conditional on the covariates and is shown to be a simple (two parameters) yet flexible (broad dispersion levels) choice compared to more commonly used distributions for count data. Moreover, its definition as a discretized continuous Weibull distribution provides a latent continuous space in the vicinity of the data with a one-to-one mapping with the inferred conditional independence graph. This may be useful in deriving theoretical properties of the proposed approach.

Thirdly, a Bayesian inferential procedure based on the extended rank likelihood and on an efficient continuous-time birth-death process allows to account for the full uncertainty both in the marginals, and thus in the effects of covariates on the microbial abundances, and in the graph component. The latter is important, particularly in high-dimensional settings where model selection methods for regularized approaches do not work well and where there is typically a large uncertainty around the optimal graph. The method proposed captures this uncertainty at the level of the graph structure (via posterior probabilities of each link) and intensity of the interactions (via posterior estimates of partial correlations), but any

other graph statistics of interest can be estimated via Bayesian averaging.

The simulation study and the real data analysis of microbiome data show the usefulness of the proposed approach at inferring networks from high-dimensional count data in general, and its relevance in the context of microbiota data analyses in particular. Indeed, the inferred interactions between firmicutes and bacteroidetes in the gut microbiota can create an opportunity for microbiome research to develop new microbial targets for the nutritional or therapeutic prevention and management of pathological conditions affecting the gastrointestinal tract, such as inflammatory bowel diseases, obesity and type 2 diabetes. At the same time, the analysis proposed has shown the potential to detect crucial interactions between the gut and oral microbiota, which has been suggested only recently in the literature.

## Funding

This project was partially supported by the European Cooperation in Science and Technology (COST) [COST Action CA15109 European Cooperation for Statistics of Network Data Science (COSTNET)].

## Software

The method proposed in this paper is implemented in the R package `BDgraph` which is freely available from the Comprehensive R Archive Network (CRAN) at <http://cran.r-project.org/packages=BDgraph>.

## References

- Behrouzi, P. and E. Wit (2019). Detecting epistatic selection with partially observed genotype data by using copula graphical models. *Journal of the Royal Statistical Society: Series C (Applied Statistics)* 68(1), 141–160.
- Burger, D., R. Schall, J. Ferreira, and D.-G. Chen (2020). A robust Bayesian mixed effects approach for zero inflated and highly skewed longitudinal count data emanating from the zero inflated discrete Weibull distribution. *Statistics in Medicine* 39(9), 1275–1291.
- Chakraborty, S. (2015). Generating discrete analogues of continuous probability distributions - A survey of methods and constructions. *Journal of Statistical Distributions and Applications* 2(1), 1–30.
- Choi, D. H., J. Park, J. K. Choi, K. E. Lee, W. H. Lee, J. Yang, J. Y. Lee, Y. J. Park, C. Oh, H.-R. Won, et al. (2020). Association between the microbiomes of tonsil and saliva samples isolated from pediatric patients subjected to tonsillectomy for the treatment of tonsillar hyperplasia. *Experimental & molecular medicine* 52(9), 1564–1573.
- Cougoul, A., X. Bailly, and E. Wit (2019). MAGMA: inference of sparse microbial association networks. bioRxiv.

- Dobra, A., A. Lenkoski, et al. (2011). Copula gaussian graphical models and their application to modeling functional disability data. *The Annals of Applied Statistics* 5(2A), 969–993.
- Dobra, A. and R. Mohammadi (2018). Loglinear model selection and human mobility. *The Annals of Applied Statistics* 12(2), 815–845.
- Friedman, J. and E. Alm (2012). Inferring correlation networks from genomic survey data. *PLoS Computational Biology* 8(9), e1002687.
- Friedman, J., T. Hastie, and R. Tibshirani (2008). Sparse inverse covariance estimation with the graphical lasso. *Biostatistics* 9(3), 432–441.
- Haselimashhadi, H., V. Vinciotti, and K. Yu (2018). A novel Bayesian regression model for counts with an application to health data. *Journal of Applied Statistics* 45(6), 1085–1105.
- HMP Consortium (2012). A framework for human microbiome research. *Nature* 486(7402), 215–221.
- Hoff, P. (2007). Extending the rank likelihood for semiparametric copula estimation. *The Annals of Applied Statistics* 1(1), 265–283.
- Indiani, C. M. d. S. P., K. F. Rizzardi, P. M. Castelo, L. F. C. Ferraz, M. Darrieux, and T. M. Parisotto (2018). Childhood obesity and firmicutes/bacteroidetes ratio in the gut microbiota: a systematic review. *Childhood obesity* 14(8), 501–509.
- Klakattawi, H., V. Vinciotti, and K. Yu (2018). A simple and adaptive dispersion regression model for count data. *Entropy* 20(2), 142.
- Kurtz, Z., C. Müller, E. Miraldi, D. Littman, M. Blaser, and R. Bonneau (2015). Sparse and compositionally robust inference of microbial ecological networks. *PLoS Computational Biology* 11(5), e1004226.
- Lauritzen, S. (1996). *Graphical Models*. Clarendon Press.
- Le Chatelier, E., T. Nielsen, J. Qin, E. Prifti, F. Hildebrand, et al. (2013). Richness of human gut microbiome correlates with metabolic markers. *Nature* 500(7464), 541–546.
- Lee, K., B. Coull, A.-B. Moscicki, B. Paster, and J. Starr (2020). Bayesian variable selection for multivariate zero-inflated models: Application to microbiome count data. *Biostatistics* 21(3), 499–517.
- Lee, K., A. Thomas, A. Bolte, J. Björk, L. Kist de Ruijter, et al. (2022). Cross-cohort gut microbiome associations with immune checkpoint inhibitor response in advanced melanoma. *Nature Medicine*.
- Lenkoski, A. (2013). A direct sampler for g-wishart variates. *Stat* 2(1), 119–128.
- Liu, H., F. Han, M. Yuan, J. Lafferty, and L. Wasserman (2012). High-dimensional semi-parametric Gaussian copula graphical models. *The Annals of Statistics* 40(4), 2293–2326.

- Liu, H., J. Lafferty, and L. Wasserman (2009). The nonparanormal: Semiparametric estimation of high dimensional undirected graphs. *Journal of Machine Learning Research* 10(80), 2295–2328.
- Liu, H., K. Roeder, and L. Wasserman (2010). Stability approach to regularization selection (StARS) for high dimensional graphical models. *Neural Information Processing Systems* 24, 1432–1440.
- Magne, F., M. Gotteland, L. Gauthier, A. Zazueta, S. Pesoa, P. Navarrete, and R. Balamurugan (2020). The firmicutes/bacteroidetes ratio: a relevant marker of gut dysbiosis in obese patients? *Nutrients* 12(5), 1474.
- Mohammadi, R., F. Abegaz, E. van den Heuvel, and E. Wit (2017). Bayesian modelling of Dupuytren disease by using Gaussian copula graphical models. *Journal of the Royal Statistical Society: Series C (Applied Statistics)* 66(3), 629–645.
- Mohammadi, R., H. Massam, and G. Letac (2021). Accelerating Bayesian structure learning in sparse Gaussian graphical models. *Journal of the American Statistical Association* 0(0), 1–14.
- Mohammadi, R. and E. Wit (2015). Bayesian structure learning in sparse Gaussian graphical models. *Bayesian Analysis* 10(1), 109–138.
- Mohammadi, R. and E. Wit (2019). BDgraph: An R package for Bayesian structure learning in graphical models. *Journal of Statistical Software* 89(3), 1–30.
- Murray, J., D. Dunson, L. Carin, and J. Lucas (2013). Bayesian Gaussian copula factor models for mixed data. *Journal of the American Statistical Association* 108(502), 656–665.
- Pedersen, H., V. Gudmundsdottir, H. Nielsen, T. Hyotylainen, T. Nielsen, et al. (2016). Human gut microbes impact host serum metabolome and insulin sensitivity. *Nature* 535(7612), 376–381.
- Peluso, A., V. Vinciotti, and K. Yu (2019). Discrete Weibull generalized additive model: an application to count fertility data. *Journal of the Royal Statistical Society: Series C* 68(3), 565–583.
- Prost, V., S. Gazut, and T. Bruls (2021). A zero inflated log-normal model for inference of sparse microbial association networks. *PLOS Computational Biology* 17(6), 1–17.
- Qin, J., R. Li, J. Raes, M. Arumugam, K. S. Burgdorf, C. Manichanh, T. Nielsen, N. Pons, F. Levenez, T. Yamada, et al. (2010). A human gut microbial gene catalogue established by metagenomic sequencing. *Nature* 464(7285), 59–65.
- Rashidi, A., M. Ebadi, D. Weisdorf, M. Costalonga, and C. Staley (2021). No evidence for colonization of oral bacteria in the distal gut in healthy adults. *Proceedings of the National Academy of Sciences* 118(42), e2114152118.



- Roverato, A. (2002). Hyper inverse Wishart distribution for non-decomposable graphs and its application to Bayesian inference for Gaussian graphical models. *Scandinavian Journal of Statistics* 29(3), 391–411.
- Roy, A. and D. Dunson (2020). Nonparametric graphical model for counts. *Journal of Machine Learning Research* 21(229), 1–21.
- Sklar, A. (1959). Fonctions de répartition à n dimensions et leurs marges. *Publications de l'Institut de Statistique de l'Université de Paris* 8, 229–231.
- Vinciotti, V., E. Wit, R. Jansen, E. Geus, B. Penninx, D. Boomsma, and P. Hoen (2016). Consistency of biological networks inferred from microarray and sequencing data. *BMC Bioinformatics* 17.
- Yang, L., E. Frees, and Z. Zhang (2020). Nonparametric estimation of copula regression models with discrete outcomes. *Journal of the American Statistical Association* 115(530), 707–720.

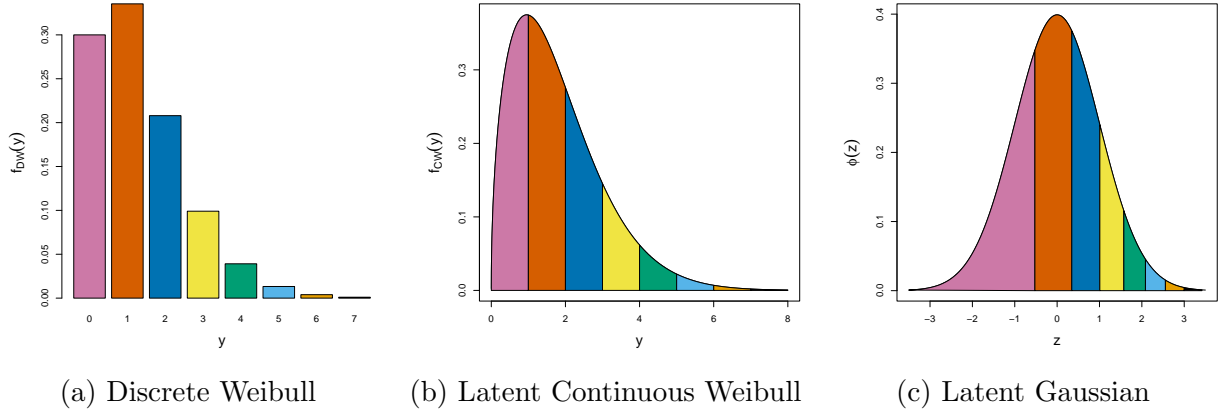


Figure 1: Schematic connection between (a) the discrete Weibull probability mass function  $f(y; q = 0.7, \beta = 1.5)$ , (b) the underlying continuous Weibull density  $f_{CW}(y; q, \beta)$  and (c) the latent Gaussian  $z = \Phi^{-1}(F_{CW}(y; q, \beta))$ . Each colour relates to the probability associated to the corresponding value (here microbial abundance) of the discrete random variable.

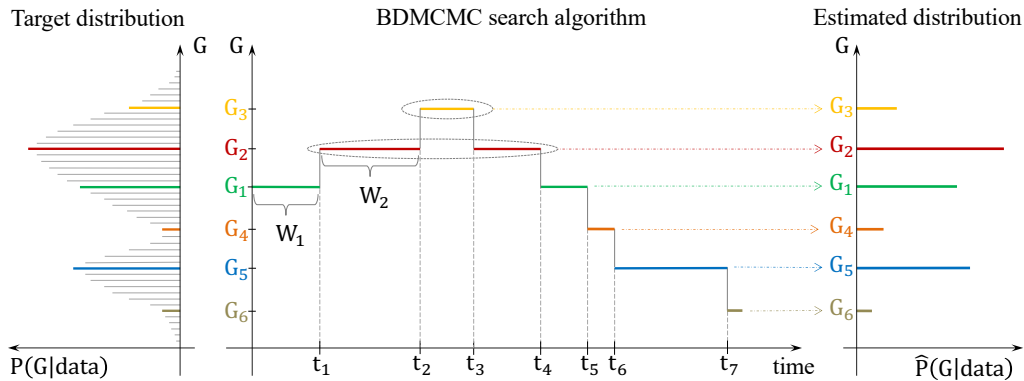


Figure 2: Graphical representation of the BDMCMC search algorithm over the graph space for the Step 2 of Algorithm 1. The left panel shows the target posterior distribution of the graphs, while the right panel represents its estimation based on the total waiting times of the graphs visited by the algorithm. The middle panel visualizes how the algorithm explores the graph space, where  $\{W_1, W_2, \dots\}$  are the waiting times and  $\{t_1, t_2, \dots\}$  are the jumping times of the algorithm. This figure is adapted from Mohammadi et al. (2021).

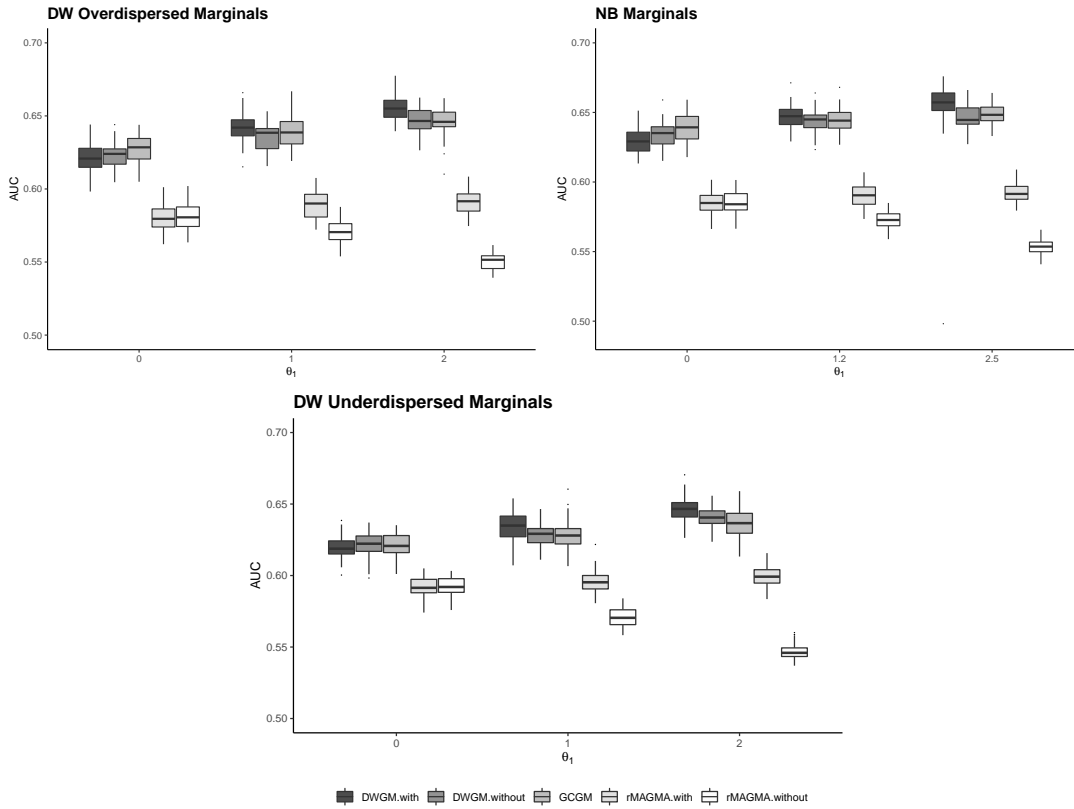


Figure 3: AUC values of network recovery on data simulated with DW and NB marginals linked to a binary covariate  $X$  via constant  $\beta$  (for DW) and  $\phi$  (for NB) parameters, but  $q$  (for DW) and  $\mu$  (for NB) parameters dependent on  $X$  through a regression coefficient  $\theta_1$ . The DWGM and rMAGMA models that account for covariates (DWGM.with and rMAGMA.with, respectively) are compared with the corresponding models with parametric marginals not dependent on  $X$  (DWGM.without and MAGMA.without, respectively) as well as with a model with non-parametric marginals (GCGM), across increasing values of  $\theta_1$ .

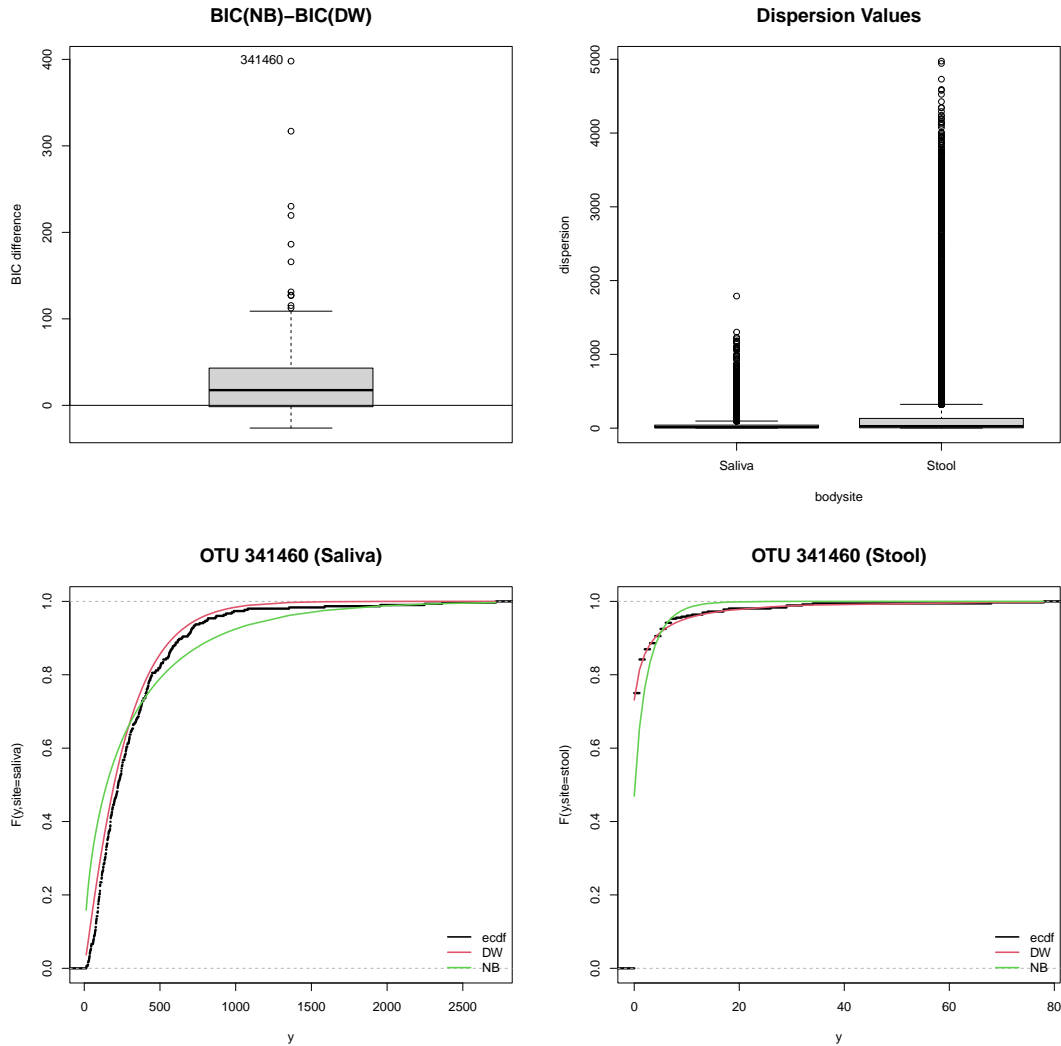


Figure 4: Top: Boxplot of BIC differences between the NB model and the DW model across all 155 OTUs (left) and dispersion levels from the fitted DW model for each OTU and each observation, split by body site (right). Bottom: Cumulative distribution functions (empirical and fitted) corresponding to each body site for the OTU where the BIC difference is largest (397.9572).

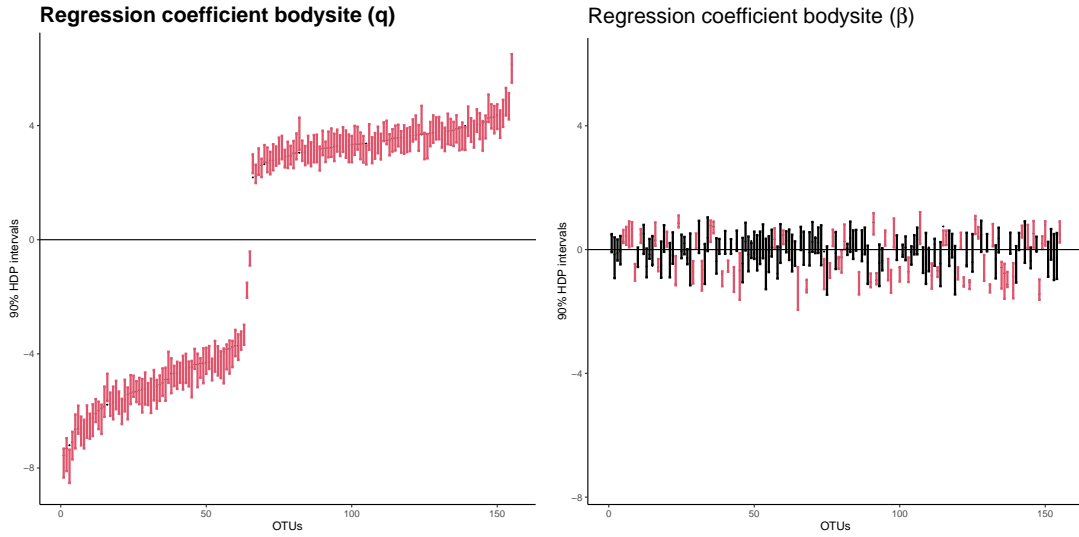


Figure 5: 90% High Posterior Density (HPD) intervals of the  $\theta$  (left) and  $\gamma$  (right) regression parameter corresponding to the body site covariate, sorted according to the median of the  $\theta$  regression coefficient across the posterior samples. Intervals that do not contain the zero are coloured in red.

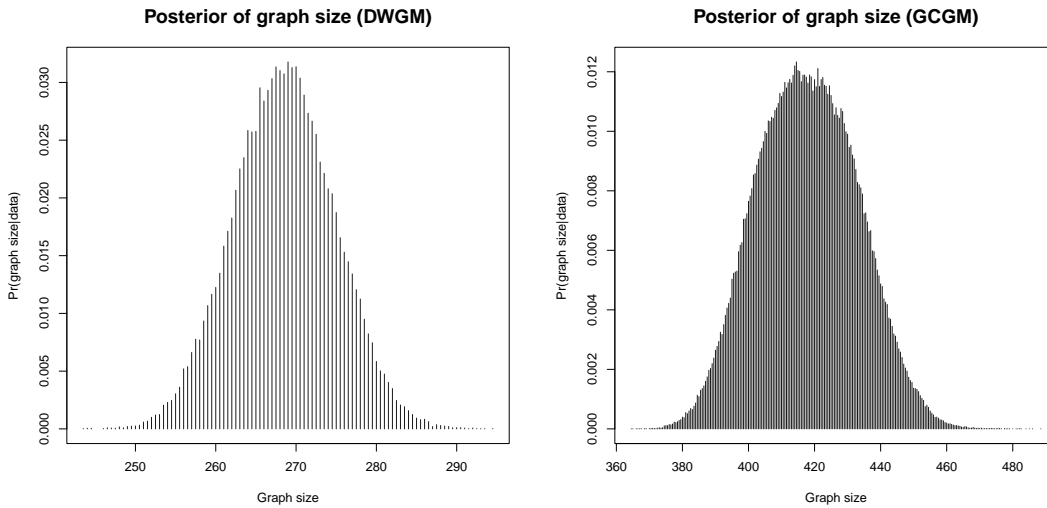


Figure 6: Posterior distribution of graph sizes for the model DWGM that accounts for covariates (left) versus the Gaussian copula graphical model that does not make use of covariates (GCGM, right).

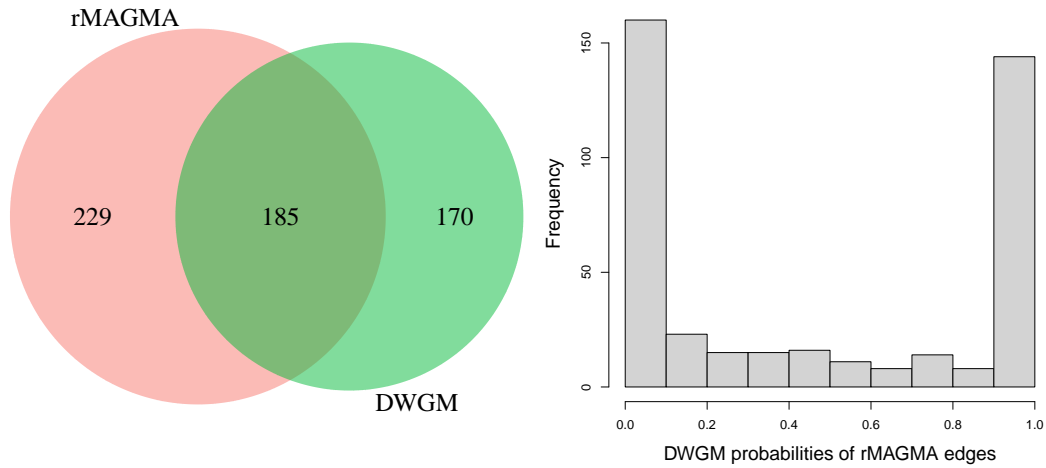


Figure 7: Left: Venn diagram comparing the optimal graph estimated by **rMAGMA** using the **stars** criterion and the optimal graph estimated by **DWGM** by setting a cutoff of 0.5 on the posterior edge probabilities. Right: Histogram of **DWGM** posterior edge probabilities associated to the 414 edges detected by **rMAGMA**.

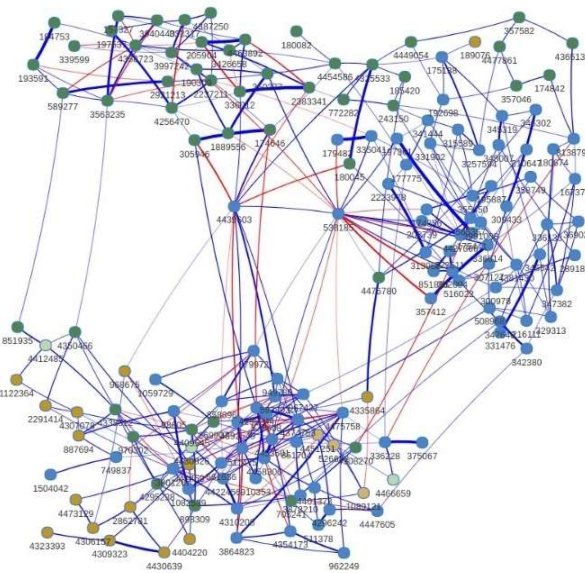


Figure 8: The inferred microbiota system with posterior edge probabilities greater than 0.5. Node colours are associated to OTU phyla, with ● Firmicutes, ● Bacterobacteria, ● Actinobacteria, ● Proteobacteria and ● Fusobacteria. Edge colors are associated to positive — and negative — partial correlations.